TOWARD CONTINUOUS AND UPDATED 3D GEOSPATIAL TERRAIN MODELLING BASED ON DEM AND LiDAR DATA

S. Dalyot, E. Keinan, Y. Doytsher

Mapping and Geo-Information Engineering, Technion, Israel Institute of Technology
Technion City, Haifa 32000, Israel
Tel. (972)48292660, Fax (972)48295708, - (dalyot, erank, doytsher)@technion.ac.il

Commission IV, WG IV/4

KEY WORDS: Spatial Analysis, Database Updating, Computer Vision, Data Integration, Topographic Mapping, LiDAR, DEM, Monitoring

ABTRACT:

The constant need for updated and accurate representation of our natural environment, which can be produced from various mapping and observation tools, is one of the major missions the geoinformation community has to provide a solution for. Digital Terrain Model (DTM) datasets that exist for the last few decades are amongst the main geospatial data widely used and applicable. Light Detection and Ranging (LiDAR), on the other hand, is relatively a newer geospatial measurement tool, which enables the quick production of the scanned surface and its coverage representation. Consequently, utilizing up-to-date and accurate datasets produced from LiDAR measurements for GIS related tasks, such as updating existing Digital Elevation Model (DEM) datasets, should be considered. Nevertheless, using simultaneously these geospatial datasets produced from various sources, which consists of different data class, requires addressing the issue of integrating data produced on different epochs. A simple 'insertion' of scattered LiDAR patches based solely on the reference coordinates systems may result in an ambiguous modelling and evident discontinuities in the produced updated terrain representation. Moreover, raw LiDAR datasets present surface features that need to be filtered out prior to the integration process. This paper presents a novel LiDAR data filtering algorithm accompanied by a two-stage hierarchical integration process. Implementing these enabled a precise global and local monitoring analysis of the inherent inconsistencies in the different datasets, which yields an accurate and continuous modelling and updating of LiDAR data within a wide DEM dataset.

1. INTRODUCTION

Nowadays, spatial topographic datasets are amongst the main resources for a variety of terrain relief and natural phenomenon analysis and research applications, such as hydrogrpahy, urban mapping, risks and damages assessments, etc. A majority of these applications are based on spatial digital datasets, which enable precise and fast geometric and visual analysis of the terrain, such as slope, flow direction, visibility-lines, and more. DEM datasets analysis is widely used and many known algorithms make use of this data type. LiDAR datasets, on the other hand, which are produced by Airborne Laser Scanner (ALS) systems, are relatively new data type for terrain relief representation. Mathematical algorithms that make use of the vast potential of this data are constantly developed. LiDAR data presents much more dense and accurate data in respect to DEM datasets: up to 16 points per $1m^2$ and position accuracy around 0.1m are now common. Consequently, LiDAR data represent in a more accurate and dense form the terrain relief, yielding a reliable and up-to-date model for updating purposes of existing topographic datasets. Nevertheless, both datasets present fundamental different data class (format, resolution, accuracy, datum, etc.). As a result, a local thorough investigation of the relative spatial correlations exist between the datasets is essential. In addition, both datasets were acquired on different epochs and were produced by different technologies. These contribute to the existence of distinct topographic changes, which further contributes to the existence of systematic and random morphologic discrepancies between both datasets (Hutchinson and Gallant, 2000). These discrepancies are categorized by two groups: global systematic ones that can be monitored and modelled; and, local random ones that can be quantified only by local rigorous analysis. As a result, a direct superimposition of a LiDAR patch into an existing wider DEM datasets, which is based solely on their reference coordinates systems, will result in an ambiguous and ill-defined modelling and updating. Alternative updating mechanisms, such as height averaging and height smoothing, will not produce better results. This is mainly because they do not implement spatial monitoring processes and ignore accuracy adjustments, which are clearly needed when the mentioned types of discrepancies exist: the updated terrain relief will appear truncated and discontinuous (artificial break-lines). Figure 1 depicts a superimposition of 0.25 points per meter resolution LiDAR data on top a 25m resolution DEM (continuous white line) showing distinctive terrain discontinuities.

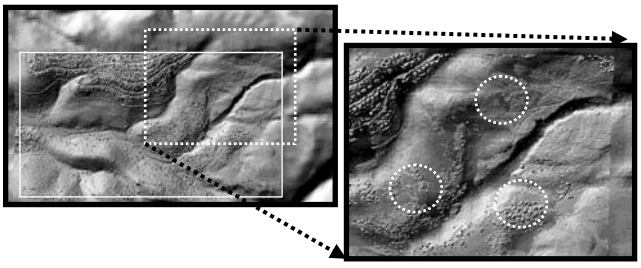

Figure 1. Spatial datasets superimposition showing truncated entities morphology, spatial ambiguity (zoomed area on the right), and planes intersections (dashed circles)

Moreover, the data represented by LiDAR data contains not only terrain features, but surface (off-terrain) features as well, such as vegetation and buildings. LiDAR data do not store semantic information regarding the scanned objects. This yields that a preliminary robust and reliable filtering algorithm on the raw LiDAR data is mandatory, in which automatic classification of terrain, trees, vegetation, buildings, etc. will take place. Vosselman (2000) suggested employing a morphological filter based on height differences among scanned points. Kraus and Pfeifer (2001) suggested dividing the scanned data into strips and then iteratively apply an interpolation to define points that belong to the DEM. Morgan and Habib (2002) proposed a region growing algorithm, which applies a least-square adjustment on the laser data linked topologically by a Triangular Irregular Network (TIN) definition.

No literature on updating DEM with up-to-date LiDAR was found. Still, the problem of integrating multiple DEM datasets with various accuracies was carried out by (Podobnikar, 2005) and (Frederiksen et al., 2004). In both studies the datasets utilized for the task were preliminary mutually geo-referenced, while a localized weighting process on the datasets' heights was implemented. Koch and Heipke (2004), and Walter and Fritsch (1999), among others, have addressed the issue of integrating DEM datasets with other types of data structures, such as 2D and 2.5D vector-data, mainly for the purpose of GIS semantic visualization. Furthermore, while vector data represent entities, such as networks or discrete data structures (points, polylines and polygons), the hypothesis of DTM geospatial datasets is that they represent continuous reality, i.e. terrain.

Recent studies implement various methods of LiDAR data - mainly terrestrial scans - and image registration. Bae and Lichti (2004) suggest using variation in curvature as the matching criterion on local points. Dold and Brenner (2006) proposed an autonomous matching based on planar patches via geometric constraints. Al-Manasir and Fraser (2006) suggest an autonomous registration supported by the placement of artificial signalized targets.

2. ALGORITHM OUTLINE

An updating process requires complete knowledge regarding the spatial relations exist between datasets. This can be achieved by implementing 3 main stages:

1. Registration (geo-referencing) - selecting a common mutual working schema (spatial reference frame) while relying on topologic relations between conjoint unique entities that exist in both datasets. This can be achieved by implementing various schemas, such as invariant property or clustering approach.
2. Matching - spatial analysis process, which uses the registration knowledge, where a qualitative reciprocity is extracted for both datasets. This enables precise and complete modelling of existing geometric conditions between datasets. The matching schema is derived from: data type and volume, its semantic and geometric characteristics, the topologic relation, and more.
3. Updating - a process that uses the quantitative matching and modelling knowledge for a correct data insertion.

In order to solve the inherent discrepancies we propose to divide the mutual coverage area into several separate homogenic topographic areas. An independent modelling process on each of these areas will satisfy the need for a precise spatial monitoring. Two-stage hierarchical process is proposed: first, implementing an accurate datasets' geo-referencing, which enables global discrepancies monitoring; then, this value is utilized for local spatial matching, which enables monitoring the local random discrepancies that still exist. Prior to this, the implementation of a novel filtering algorithm is carried out on the raw LiDAR data, which results in an accurate and reliable representation of the terrain relief. The complete stages of this process - from global to local, as depicted in Figure 2 - validates that the updated representation preserves the geometry of existing features and their topology, while preventing the existence of distortions. In the next section the concept and contributions of the proposed automated two-stage hierarchical updating process are outlined; experimental results and the conclusions sections are given afterwards.

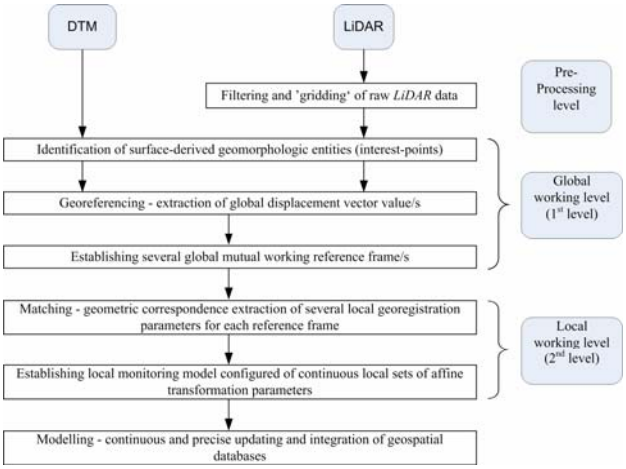

Figure 2. Block diagram of the proposed procedure

2.1 Pre-Processing

As mentioned earlier, raw LiDAR data contains surface representation, i.e., objects, so a filtering process is required. The purpose of a filtering process is to predict - according to a specific set of geometric rules - the terrain relief. This translates to a classification process, in which every LiDAR point is categorized into one of two groups: terrain; and, off-terrain. Here, the implementation of high degree orthogonal polynomials was carried out (Abo-Akel et al., 2007). The use of orthogonal polynomials makes it possible to predict with high certainty a continuous representation of the terrain from the data, and hence classify off-terrain points, which lie at a certain distance from the predicted terrain. This technique is not sensitive to noise, data-errors, truncated and singular data.
The orthogonal polynomials are two-dimensional, thus the data was divided into strips along the primary and secondary axes (the stripes' width is derived by the data density). A set of polynomials are orthogonal over a set of points $\{x_i\}$ if the condition in Equation 1 is met.

$$\sum_{i=1}^{n} w(x_i) \cdot P_j(x_i) \cdot P_k(x_i) = 0 \qquad \forall\ j \neq k \tag{1}$$

where i is the index of the points set, j and k are the indexes of the polynomials p, and w is a weighting function.

Points' classification is based on the residuals between the measured heights and the extracted orthogonal polynomials' calculated heights. This translates to terrain points, which are characterized with a negative residual (or a relatively small positive residual); and, off-terrain points, which are characterized with a positive residual. Hence, the weight of the points should be updated iteratively during the process. Here, we suggest using a weighting function, depicted in Equation 2.

$$w = \begin{cases} 1 & dh_i \le th \\ 1 - \left(\frac{dh_i}{Th} \right)^2 & th < dh_i \le Th \\ 0 & dh_i > Th \end{cases} \quad (2)$$

where dh_i is the height residual, and th and Th are the minimum and maximum thresholds, respectively.

The process initiates with high degree orthogonal polynomials, while their degree is reduced each iteration. As the process progresses, the polynomial becomes a better representation of the terrain, i.e., the residuals are small. The process convergent when the number of filtered off-terrain points in a certain iteration is larger than the one in the previous iteration. This indicates that the polynomial describes a smoothed version of the terrain description. The points that were filtered in the last iteration are added as terrain points. When the process terminates on both axes a point can be classified as terrain only if it is classified as one simultaneously.

In addition to implementing this mechanism, the execution of a morphological filtering process is carried out. This process is designated to examine off-terrain points that were erroneously classified as terrain points. The morphological filter is based on height and distance differences. Each classified terrain point is examined in relation to its neighborhood at a given distance. The neighboring points are chosen based on TIN topology. If the majority of neighboring points are classified as off-terrain points and the height difference is below a certain threshold, then the classification of the point is changed from terrain to off-terrain. The outcome of this complete algorithm is LiDAR points that are classified as terrain with high level of certainty.

2.2 Interest Points Extraction

The geo-referencing process is carried out while relying on sets of unique selective homologous features. Here, we referred to distinctive interest points in the topography. A novel extraction mechanism of surface-derived geomorphologic maxima unique features, such as local hill peaks, was implemented (Dalyot and Doythser, 2006). This mechanism is based on designated geometric, topologic, and topographic conditions. A generalization algorithm for interest area recognition is established by constructing four local second degree polynomials around each grid-point - one for each principal direction. These polynomials represent a generalized version of the point's topographic surroundings, making it possible to extract local maxima, as depicted in Figure 3. It is worth noting that this mechanism is implemented on grid-domain. As a result, in this stage the filtered LiDAR data was gridded (it should be emphasized that this is the only occurrence where an interpolation was carried out on LiDAR data, and all the other algorithms and processes preserved and utilized its raw data structure).

2.3 Geo-Referencing

In order to extract a coarse reference frame, a geo-referencing process is executed on the selective homologous interest points identified in both datasets. The suggested process relies on the Hausdorff distance algorithm, which does not require any constraints or a-priori knowledge on the points' dispersal or their topologic relations. Given two sets of points $A = \{a_1,\ldots,a_m\}$ and $B = \{b_1,\ldots,b_n\}$, the forward Hausdorff distance - h - measures the degree of mismatch between the two sets, as defined in Equation 3 (Huttenlocher et al., 1993). This equation identifies point $a \in A$ that is farthest from any point in B, and then measures the distance from a to its nearest neighbor b in B. This Euclidean spatial distance gives an initial estimation of the global registration value, which is statistically evaluated by the correspondence it obtains between the remainder points in sets A and B.

$$h(A,B) = \max_{a \in A} \min_{b \in B} \|a - b\| \quad (3)$$

The minimum number of paired-up points required is derived from the transformation model used in the geo-referencing process. Here, we referred to 3D translation vector: dx^0, dy^0, and dz^0, while requiring at least 4 pairs to obtain a statistical evaluation of the standard deviation values.

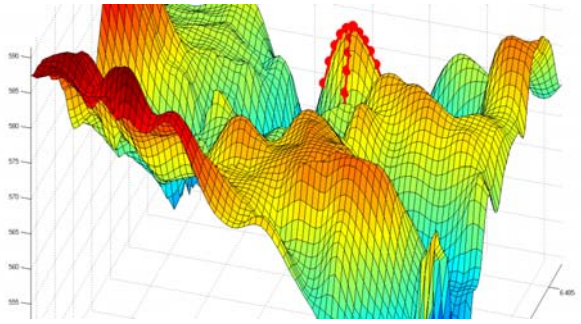

Figure 3. Four polynomials (bold red lines and dots) representing a generalized version of topographic surroundings

2.4 Local Matching

The registration value extracted gives knowledge on the 'global' reciprocal working reference frame, thus enabling the implementation of an adequate matching process on homologous corresponding local data frames divided from the complete mutual coverage area. It is obvious that by matching small frames more effective monitoring and modelling of the local random incongruities, i.e., inherent 'errors' exist between the datasets, is feasible. Monitoring errors is achieved by minimizing the target function, i.e., extracting the best possible correspondence between the datasets. The geometric target function implemented is defined by a spatial transformation model. In this research, a constrained ICP algorithm (Besl and McKay, 1992) was implemented independently on each local frame, which was derived from the constraints that the data characteristics and problem imposed.

Three geometric constraints were implemented in the ICP process - outlined in Equation 4 - to assure that the nearest neighbor search criteria will be achieved correctly and fast between two homologous local frames. These constraints verify that each of the paired-up points is the closest one exists, as well as having the same relative topography surroundings. Moreover, the algorithm was modified so it could suit the different data formats, i.e., structures: TIN vs. grid. It is worth emphasizing that the two datasets will usually present significant point density disparity that can reach up to 1:1000 (DEM vs. LiDAR) in a single ICP matching frame. As a result, it was decided to match each LiDAR point to its corresponding DEM point. This allowed the preservation of the high resolution and accuracy of the LiDAR observations.

$$
\begin{aligned}
Z_i^g &= \frac{h_1}{D}\cdot X_i^g + \frac{h_3}{D}\cdot Y_i^g + \frac{h_4}{D^2}\cdot X_i^g \cdot Y_i^g \\
Z_i^g &= -\frac{h_4 \cdot y_f^{'}}{D^2}\cdot X_i^g + \frac{h_3}{D}\cdot Y_i^g + \frac{h_4}{D^2}\cdot X_i^g \cdot Y_i^g + \left(z_f^{'} - \frac{h_3 \cdot y_f^{'}}{D} \right) \\
Z_i^g &= \frac{h_1}{D}\cdot X_i^g - \frac{h_4 \cdot x_f^{'}}{D^2}\cdot Y_i^g + \frac{h_4}{D^2}\cdot X_i^g \cdot Y_i^g + \left(z_f^{'} - \frac{h_1 \cdot x_f^{'}}{D} \right)
\end{aligned}
\qquad (4)
$$

where h_1 to h_4 are calculated from the height of local DEM grid cell corners: Z_1 to Z_4 ($h_1=Z_1-Z_0$, $h_2=Z_2-Z_0$, $h_3=Z_3-Z_o$, $h_4=h_2-h_1-h_3$); D denotes the DEM grid resolution; G and F denotes the datasets DEM and LiDAR, correspondingly; (X^g_i, Y^g_i, Z^g_i) denotes the paired-up nearest neighbor in G; and, ($x_f^{'}$, $y_f^{'}$, $z_f^{'}$) denotes the transformed point from dataset F.

The transformation model implemented in the matching process is composed of three translation parameters: dx, dy, and dz. Based on the assumption that both datasets are already registered northward, the three rotation angles: φ, κ, and ω are ignored, because their values are almost zero (if required, the rotation angles can easily be added to the transformation model). Every zonal ICP process used the registration value extracted in the geo-referencing stage as the approximated translation vector, i.e., dx^0, dy^0, and dz^0.

Each matching set includes three geo-registration parameters (i.e., transformation, which in this case is equivalent to spatial translation) that best describe the relative spatial geometry of the mutual homologous frames that were matched. Since this process yields better localized geo-registration definition, it ensures matching continuity on the entire area (as opposed to matching the entire data in a single matching process), as well as excluding local minima solution for the ICP process. These geo-registration sets can be described as elements stored in 2D matrix: each set is stored in the cell that corresponds spatially to the homologues frames it belongs to (Dalyot and Doythser, 2007). This data structure contributes to the effectiveness of the integration and updating processes.

2.5 DEM Update

Knowing the complete and accurate sets of local spatial relations enables the implementation of an update process. Still, the resolution and data-structure of the geo-registration matrix and both datasets are different. In order to preserve continuous modelling - semantically and topologically - as well as correct updating, an interpolation has to be carried out on the matrix's values in order to preserve the datasets denser resolution. The implementation of bi-directional third-degree parabolic interpolation was carried out (Doythser and Hall, 1997). For all LiDAR points the precise corresponding transformation parameters are calculated via the interpolation algorithm in respect to their location within the matrix cells and the geo-registration values these cells store. These transformation values are then used to calculate the correct and accurate location of the LiDAR points within the DEM dataset - hence an updating process is achieved.

3. EXPERIMENTAL RESULTS

The proposed mechanism was tested on several datasets - synthetic and real. An evaluation of the filtering algorithm was carried out derived by the effectiveness of terrain points identification. Figure 4 depicts a side-view of LiDAR strip while using the proposed filtering algorithm. By examining this figure it is obvious that the polynomial (continuous black line) represents adequately the terrain while filtering the surface objects: building (in the middle), and vegetation (scattered).

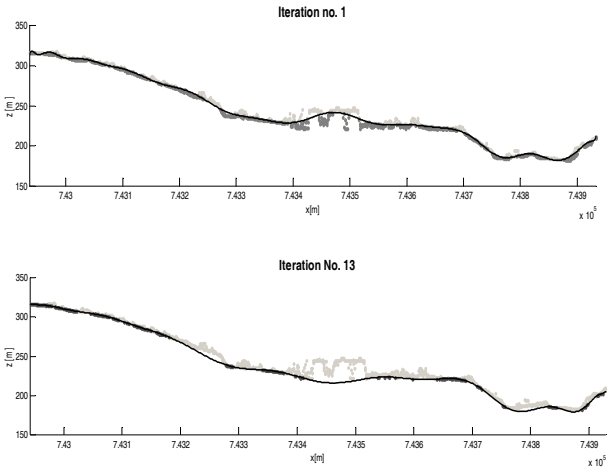

Figure 4. Initial and final filtering stages: dark-grey points depict terrain points; light-grey points depict filtered objects; black line depicts calculated polynomial (values in meters)

Figure 5 depicts an area before and after the implementation of the proposed filtering algorithm. The upper figure shows buildings as well as vegetation that were filtered - as depicted in the lower figure. Though a filtering process was carried out, it is visible that after a hole-filling interpolation process that was carried out the topography is still continuous, and that roads, which are part of the terrain representation, remained intact (lower image top-left corner).

A complete update process was carried out on a DEM with 25m resolution, which was based on a digitization of 1:50K contour maps (produced approximately 20 yrs ago), and a LiDAR scan that presented 0.25 points per $1m^2$ (collected in recent campaign). The mutual area presented in both datasets covered approximately 3 km^2. The automatic interest points extraction proved to be geo-morphologically accurate and precise - both in the DEM and LiDAR datasets - while achieving sub-cell resolution, which improved the reliability of the geo-referencing process. Total of 48 interest points were extracted in the DEM dataset, and 7 in the LiDAR. Figure 6 depicts a section within the mutual area with extracted interest points in both datasets.

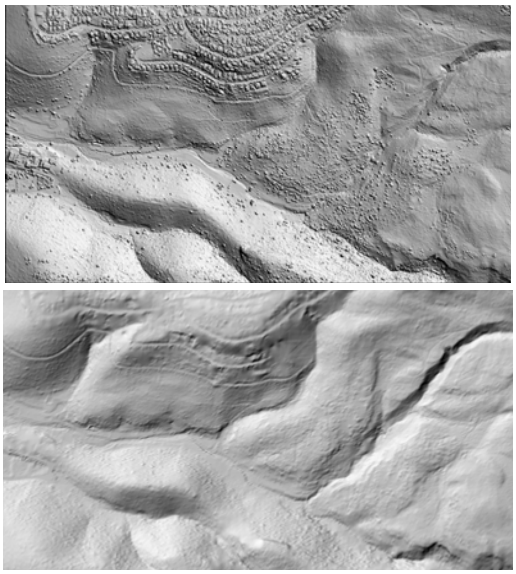

Figure 5. A shaded relief representation of LiDAR scan (up); and, the outcome of the proposed filtering algorithm (down)

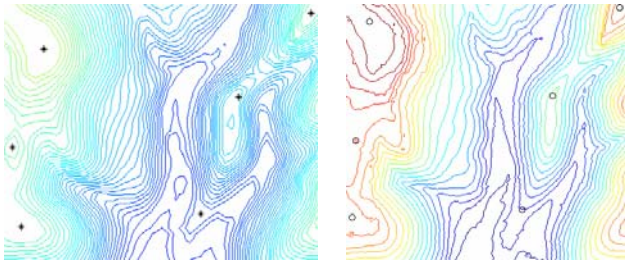

Figure 6. Contour representation of the same coverage area (DEM on the left and LiDAR on the right) depicting the reliability of the interest points identification process

The forward Hausdorff distance algorithm proved to be robust and fast, while it succeeded in extracting the correct global inconsistencies exist between the DEM and LiDAR. Out of several hundred possible couplings, the algorithm was able to identify 4 pairs with similar reciprocal spatial relations. The calculated geo-referencing vector values were: 9.3m in *X* direction, 15.6m in *Y* direction, and 3.0m in *Z* direction. The standard deviation for *X* and *Y* values was less than ±3m. A visual inspection of the datasets verified these values.

The entire DEM dataset was composed of 40,401 points, while the LiDAR had more than 630,000 points. Within the mutual coverage area the DEM had less than 3,800 points, which translates to a ratio of 1:165 (DEM vs. LiDAR). After the filtering process, the LiDAR dataset presented more than 510,000 points, which translates to a ratio of 1:135. The matching process was carried out separately and independently on 100x100m frames (approximately 200 frames). The ratio between the LiDAR and DEM number of points in each frame varied between 1:165 (a frame with almost no filtered points) and 1:2 (a frame with massive filtering). As will be proved later - there was a clear correlation between this ratio value and the reliability and accordance of the matching process. A frame that had gone through a massive filtering process suffered from positioning uncertainty of the remaining points, and had low signal to noise ratio. As a result, the matching process did not achieve a qualitative matching, i.e., frames with no 'spatial accordance'. This phenomenon is a result of massive time dependent morphologic changes that had gone in that area, or the fact that a certain area is dominated by surface objects.

Figure 7 depicts the values that were extracted in the matching process for all frames. It is clear that the local matching values for most frames are similar to the initial geo-referencing value used in the process. The value of *dz*, on the other hand, showed inconsistencies within the entire area. This can be explained by the spatial relations between the datasets that showed rapid height changes - one plane intersecting the other. Moreover, it is evident that frames that show matching values anomalies are frames that had gone massive filtering or morphologic changes. A statistical test was carried out on the values extracted to evaluate their correctness in respect to the given topographic conditions. Each LiDAR point was transformed while using the transformation values calculated via the proposed interpolation on the geo-registration matrix values. The calculated height was then compared to the DEM height at that same position. The average of all the differences values per frame - *z_avr* - gave a qualitative statistical evaluation for the transformation values extracted. By inspecting top row of Figure 8 it is evident that other than several frames that showed relatively high *z_avr* values, all the other frames showed values between (-3)m and 3m - a value that is smaller than the estimated 5m accuracy of the DEM. More than 85% of all the frames showed these values. Moreover, the standard deviation of *z_avr* was calculated - *z_std*, which in most frames was less than 3m. If *z_avr* and *z_std* were re-calculated based only on the frames that had gone thorough relatively small filtering process, these values were 0m and 1-2m, correspondingly. Another statistical evaluation was the number of coupled points in the matching process for each frame. This number was much smaller in frames that had gone thorough filtering process - almost half the number in respect to other frames. It is worth emphasizing that when an alternative geo-referencing value was used in the ICP matching process, *z_avr* and *s_std* were much higher - reaching up to 20m - as shown in lower row of Figure 8. This fact emphasizes the significance of using a correct geo-referencing vector to the completeness of the updating process.

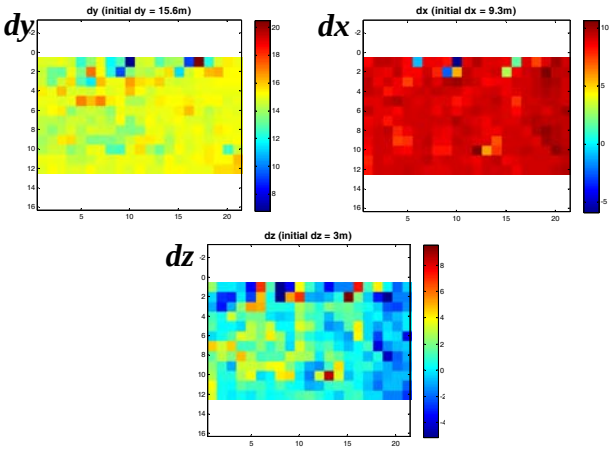

Figure 7. Transformation values calculated in the matching process (color bar values in meter)

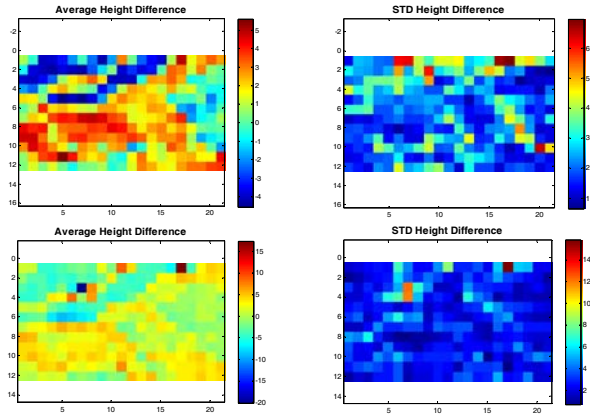

Figure 8. Statistical values: *z_avr* and *z_std*. 1st row - using the extracted geo-referencing vector in ICP process; 2nd row - using an alternative value (color bar values in meter)

The data in the LiDAR dataset can now be superimposed onto the existing DEM dataset in its correct and precise position. First, the heights of the filtered points are re-calculated while relying on the orthogonal polynomials extracted that pass through them. Then, for each LiDAR point a local-precise 3 transformation parameters are calculated while relying on the bi-directional third-degree parabolic interpolation. Figure 9 depicts the hybrid and updated dataset that is the result of these stages. It is clear that the topology of the LiDAR and DEM data - as well as among them - is fully preserved representing continuous entities on both sides of the mutual coverage area.

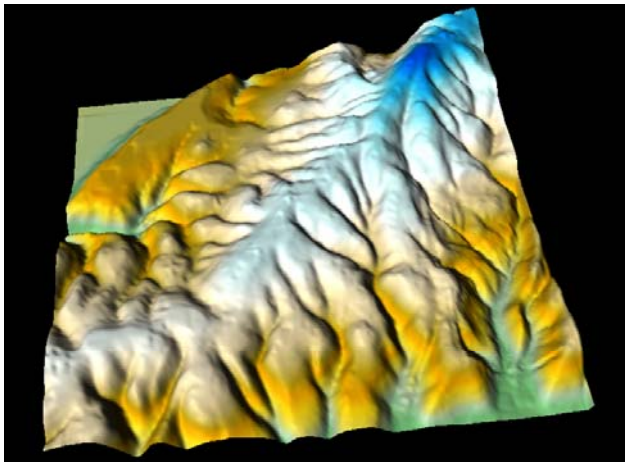

Figure 8. 5m resolution hybrid DEM dataset covering approx. 25km^2 - LiDAR dataset superimposed in lower-right region

4. CONCLUSIONS

Updating geo-spatial DTM datasets that have different data structures and were acquired on different observations epochs demand local and precise monitoring procedures of their mutual topology. This is vital for a correct modelling of their inherent relations and inconsistencies. Only then, the preservation of their inner morphology, and hence the production of an accurate, reliable and continuous updated terrain representation is feasible. The approach suggested here, starting with the implementation of a robust and reliable filtering algorithm on LiDAR data; and, continue with an adequate geo-referencing and local matching processes that preserve each of the datasets inner data-frame assure a reliable and correct updating process.

Although no a-priori information or approximation regarding the relative position of the datasets is required, the method and its implementations are fully automatic. The extraction of interest-points in both datasets was successful - in terms of topographic accuracy and topographic morphology. Matching TIN and grid datasets yielded new algorithms and constraints implementation, resulting in correct spatial datasets modelling that preserved local geometric features and their topological relations, while preventing distortions.

It was concluded that in dense vegetation or urban areas, a massive filtering process might result in a small signal to noise ratio. This may result in a process that is not reliable enough due to data defects. These areas will require local handling on latter stage.

The mathematical concepts and algorithms presented here can be utilized with minor modifications to other spatial models, as well as analysis of terrain alterations that are time-derived, such as monitoring natural phenomenon, risks and damages assessments, etc.

REFERENCES

Abo-Akel N., Filin S., and Doytsher, Y., 2007. Orthogonal Polynomials Supported by Region Growing Segmentation for the Extraction of Terrain from LiDAR Data. *Photogrammetric Engineering & Remote Sensing*, 73(11): pp. 1253-1266.

Al-Manasir K., Fraser C.S., 2006. Registration of terrestrial laser scanner data using imagery. *Phot. Rec*. 21, pp. 255–268.

Bae K., Lichti D., 2004. Automated Registration of Unorganised Point Clouds From Terrestrial Laser Scanners. *Int. Arch. of Photogrammetry, Remote Sensing and Spatial Information Sciences* 35 (Part B5), pp. 222–227.

Besl P. J., McKay N. D., 1992. A Method for Registration of 3-D Shapes. In: *IEEE Transactions on Pattern Analysis and Machine Intelligence*, Vol. 14, No. 2, pp. 239-256.

Dalyot S., Doytsher Y., 2007. A New Concept for Dynamic Handling of Localized Georegistration Parameters between Two Geospatial Datasets. *International Conference on Information Reuse and Integration*, IRI 2007, IEEE, pp. 429-435.

Dalyot S., Doytsher Y., 2006. A Hierarchical Approach toward 3-D Geo-Spatial Terrain Merging. *ISPRS Int. Archives, Commission IV Symposium*, Volume XXXVI part 4.

Dold C., Brenner C., 2006. Registration of Terrestrial Laser Scanning Data using Planar Patches and Image Data. *International Archives of Photogrammetry, Remote Sensing and Spatial Information Sciences* 36 (Part 5), 25–27.

Doythser Y., Hall J. K., 1997. Interpolation of DTM using bi-directional third-degree parabolic equations, with FORTRAN subroutines. *Computers and Geosciences*, Volume 23, Number 9, pp. 1013-1020(8).

Frederiksen P., Grum J., and Joergensen L.T., 2004. Strategies for updating a national 3-D topographic database and related geoinformation. *Proc. ISPRS* XXth Congress, Com. WG II/IV.

Hutchinson, M. F., Gallant, J. C., 2000. Digital Elevation Models and Representation of Terrain Shape. Wilson, John P. & Gallant, John C. (ed.), Terrain Analysis: Principles and Applications, John Wiley & Sons, Inc., pp. 29-50.

Huttenlocher, D. P., Klanderman G. A., and W. J. Rucklidge., 1993. Comparing images using the Hausdorff distance. *IEEE Trans. Pattern Intelligence & machine intelligence*, 9:850-863.

Koch, A. Heipke, C., 2004. Semantically correct 2.5D GIS data - the integration of a DTM and topographic vector data. Fisher, P., Ed., in Developments in Spatial Data Handling, Berlin, Springer, pp. 509.

Kraus K., Pfeifer N., 2001. Advanced DTM Generation from LiDAR Data. *Proceedings of ISPRS*, Commission III WG3 Symposium, Annapolis, Maryland.

Morgan M., Habib A., 2002. Interpolation of LiDAR Data and Automatic Building Extraction, Proceedings of 2002 ACSM Annual Conference.

Podobnikar T., 2005. Production of integrated digital terrain model from multiple datasets of different quality. *Int. Journal of Geographical Information Science*, Vol. 19, No. 1, pp. 69.

Vosselman G., 2000. Slope Based Filtering of Laser Altimetry Data. *IAPRS - the International Archives of Photogrammetry and Remote Sensing*, 33(B3/2):pp. 935-942.

Walter, V. Fritsch, D., 1999. Matching spatial data sets: a statistical approach. *Int. J. of geographical information science*, Vol. 13, No. 5, pp. 445.